Evaluation of Seismic Torsional Response of Base Isolated Buildings

Kazushi SHIMAZAKI
Kanagawa University, JAPAN

ABSTRACT:
The causes of torsional responses in base-isolated buildings are the eccentricity of the building's superstructure, eccentricity of isolation members, and the torsional input. The torsional response behaviors caused by eccentricity were examined. However, the behavior of isolated buildings subject to torsional motion is not clear. This paper examines the torsional response behavior of base-isolated buildings vibrating under various input motions at both ends of the building defined as phase-lagged motions or motions amplified by different subsurface layer depths. The torsional response is investigated by numerical analysis compared with the main horizontal axial displacement, and it is observed that the maximum horizontal drift at the building's end increased 20~30 percent. In order to roughly estimate torsional response, the torsional response spectrum is evaluated. The maximum drift at the building's end can be evaluated using the torsional angle and displacement spectrum.

Keywords : Base isolated building, Earthquake Resistant Design, Torsional vibration

1. INTRODUCTION

The causes of torsional responses in base-isolated buildings are:
1) Eccentricity of the building's superstructure (eccentricities of weight, rigidity, and horizontal strength)
2) Eccentricity of isolation members (eccentricities of rigidity and strength, phase lag of damper, difference in yield displacement caused by thermal and drying shrinkage[Shimazaki 2002], etc.),
3) Torsional input motion (eccentricity of foundation, phase lag of input motion, variant input caused by inclination of bearing layer).

The torsional response behaviors caused by 1) and 2) above are examined using mathematical and numerical analysis. However, the behavior of isolated buildings when the torsional motion inputs caused by eccentricity of foundation, phase lag of input motion, or variant input motion resulting from inclination of the bearing layer is not clear.

This paper examines the torsional response behavior of base-isolated buildings vibrating by the variant input motion at both ends of the building. The two types of unsynchronized motions used as input motions at both ends are defined as:
1) Phase-lagged motions dependent on building length and wave speed (Figure 1a),
2) Motions amplified by different subsurface layer types and depths (Figure 1b).

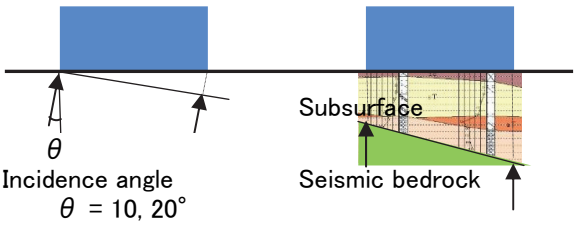

(a) Phase lag (b) Inclined bearing layer

Figure 1. Multiphase input motion

Numerical analyses are conducted to investigate the torsional response for base-isolated buildings using the parameters of building length, subsurface layer type and depth, and the type and magnitude of the input motion. The analytical models of the superstructures are flat grid frame models with the masses of the superstructure concentrated at each node without eccentricity.

Finally, a simple method to estimate the torsional response is evaluated using the torsional response spectrum calculated from the torsional angular acceleration obtained from the difference in the input seismic motion at both ends. This produces three response spectrums, namely the torsional angle, torsional angle velocity and torsional angle acceleration response spectrums.

2. ANALYTICAL MODEL

2.1. Building model

The analytical models used in this study are eight-story buildings with three bays in the span direction and three, nine, and 18 spans in the longitudinal direction with spans of eight meters as shown in figure 2. Each building has a floor plan of 24 m × 24 m, 72 m, or 144 m, surrounded by a one-meter wide balcony. The weight is assumed to be 13 kN/m^2 for each floor. The models consist of two layers – the lower one being the base layer, while the other upper one is the superstructure frame. The base layer is supported with a fixed boundary at both ends, Point A and Point B. The superstructure is assumed to be a horizontal plane frame and the total weight of each column is positioned at each node of the plane frame. The stiffness of the beam in this plane frame is set with very large values in consideration for the rigidity of the slab.

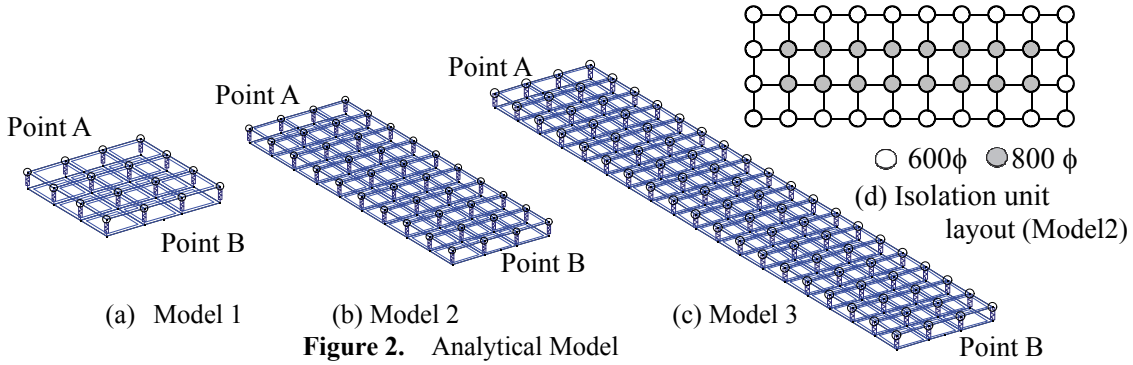

Figure 2. Analytical Model

The base isolation units are assumed to be Lead Rubber Bearings (LRB) set at each node with 600ϕ around the periphery and 800ϕ in the central area depending on the loading weight, as shown in Fig. 2d. The upper frame is supported by 16~76 base isolation units in each model. The properties of the base isolation units are shown in Table 1. The LRBs are modeled as a Multiple Shear Spring (MSS) model with four springs using the modified bilinear model prepared in the SNAP-V5 program used in this study.

Table 1. Basic assumed characteristics of LRB

Diameter[mm]		Stiffness[kN/mm]		Yield strength [kN]
External	Lead plug	Initial	Secondary	
600ϕ	120ϕ	8.32	0.83	94.2
800ϕ	160ϕ	14.8	1.48	167.6

2.2. Input motions

For buildings with rigid foundations, the input motion is averaged, and the effect of the phase lag becomes small [Yamamura 2004]. In this study, input motions are applied to the two fixed boundaries at both ends, A and B, independently. This is assumed to be the most stringent condition. In actual buildings, the phase difference effect is considered to be less than those obtained in this paper.

2.2.1 Phase lag of input motion

The parameters considered are the incidence angles as the phase lag and type of ground motions. Two incidence angles are set: θ = 10, 20 degrees as shown in Figure 1a. The phase lag time is calculated using this incidence angle on the assumption of a 100-m/s shear wave velocity. The ground motion input is applied to Point A first and then to Point B after a certain interval. Three ground motions are used, including the recorded motions of El Centro 1940 NS, Hachinohe 1968 EW, and Kobe 1995 NS, with maximum velocities of 25, 50, and 75 cm/s.

2.2.2 Inclination of bearing layer

The input ground motions are calculated using the equivalent linear analysis "SHAKE" program with simulated seismic waves at engineering bedrock as per the common Japanese target spectrum for a severe earthquake with a certain motion phase. The parameters are incidence angles of the bearing layer, types of geological layers, and types of motion phases. The incidence angle θ is set at three values; 0, 10, and 20 degrees. Three kinds of geological layer as shown in Table 2 are assumed: 1) Sandy stratum, 2) Soft ground, and 3) Deep stratum with a mid-depth gravel layer. The soil properties and depth of each layer assume the values shown in Table 2 with reference to the drilling survey data of Kanagawa prefecture, Japan. Three types of motion phases are used, namely the El Centro 1940 NS phase, Hachinohe 1968 EW phase, and a random phase. Input motions are calculated as per independent horizontal soil layer. Actual input motions are interrelated to each other and different from this assumption. In this study, this relationship was ignored and this assumption is the maximum difference boundary.

Table 2. Soil layer properties

	Point A		Point B									
			Building length	24m			72m			144m		
	Soil type	Depth (m)	slope of bearing layer / Soil type	Depth(m)								
				0	10	20	0	10	20	0	10	20
sand stratum		0		0	0	0	0	0	0	0	0	0
	fill	1.5	fill	1.5	1.5	1.5	1.5	1.5	1.5	1.5	1.5	1.5
	sandy clay	6.5	sandy clay	6.5	6.5	6.5	6.5	6.5	6.5	6.5	6.5	6.5
	fine sand with clay	8.2	fine sand with clay	8.2	8.2	8.2	8.2	8.2	8.2	8.2	8.2	8.2
	fine sand		fine sand	9.5	9.5	10.1	9.5	10.6	12.5	9.5	12.2	15.8
			clay	10.7	11.3	12.7	10.7	14.0	18.3	10.7	17.9	26.2
			fine sand with clay	11.2	13.8	16.3	11.2	18.7	26.5	11.2	25.6	40.8
	fine sand	11.9	fine sand	11.9	14.9	17.9	11.9	20.8	30.1	11.9	29.1	47.2
			Coarse sand with gravel	12.4	17.2	21.3	12.4	25.1	37.7	12.4	36.2	60.6
	gravel	13	gravel	13	18.2	22.7	13.0	27.0	40.9	13.0	39.3	66.4
Soft ground		0		0	0	0	0	0	0	0	0	0
	fill	2.6	fill	2.6	2.6	2.6	2.6	2.6	2.6	2.6	2.6	2.6
	sandy silt	4.1	sandy silt	4.1	4.1	1.5	4.1	1.5	1.5	4.1	1.5	1.5
			fine sand with clay	4.9	6.3	5.2	4.9	6.1	9.1	4.9	8.9	14.8
			fine sand	5.6	9.5	10.7	5.6	12.8	20.0	5.6	19.6	34.1
			silty fine sand	6.2	11.7	14.5	6.2	17.4	27.6	6.2	26.9	47.3
	sand	6.9	sand	6.9	15.9	18.7	6.9	21.6	31.8	6.9	31.1	51.5
	silty fine sand	10.8	silty fine sand	10.8	19.8	22.6	10.8	25.5	35.7	10.8	35.0	55.4
	sandy silt	16.2	sandy silt	16.2	25.2	28.0	16.2	30.9	41.1	16.2	40.4	60.8
	silt	20	silt	20	29.0	31.8	20.0	34.7	44.9	20.0	44.2	64.6
	sandy silt	23.3	sandy silt	23.3	32.3	35.1	23.3	38.0	48.2	23.3	47.5	67.9
			fine sand	25.2	34.8	39.3	25.2	43.2	56.8	25.2	55.9	83.0
	sandy mudstone	32	sandy mudstone	32	36.2	40.7	32.0	44.7	58.2	32.0	57.3	84.4
Intermediate gravel layer		0		0	0	0	0	0	0	0	0	0
	topsoil	1.7	topsoil	1.7	1.7	1.7	1.7	1.7	1.7	1.7	1.7	1.7
	organic silt	10	organic silt	10	10	10	10	10	10	10	10	10
			coarse sand	11.2	12.3	13.5	11.2	14.6	18.3	11.2	18.1	25.5
			silt	11.8	14.2	16.5	11.8	18.4	25.2	11.8	24.8	38.3
	sandy silt	12.5	sandy silt	12.5	16.7	19.0	12.5	20.9	27.7	12.5	27.3	40.8
	fine sand	15	fine sand	15	19.2	21.5	15.0	23.4	30.2	15.0	29.8	43.3
	silty fine sand	17.4	silty fine sand	17.4	21.6	23.9	17.4	25.8	32.6	17.4	32.2	45.7
	fine sand	24.4	fine sand	24.4	28.6	30.9	24.4	32.8	39.6	24.4	39.2	52.7
	gravel	28.4	gravel	28.4	32.6	34.9	28.4	36.8	43.6	28.4	43.2	56.7
			Coarse sand with gravel	30.2	34.2	37.3	30.2	40.0	49.4	30.2	48.8	67.5
			fine sand	32.1	36.8	41.3	32.1	45.2	58.8	32.1	57.9	85.0
	silt	35.2	silt	35.2	39.4	43.9	35.2	47.9	61.4	35.2	60.5	87.6
	tuffaceous silt	41.5	tuffaceous silt	41.5	45.7	50.2	41.5	54.2	67.7	41.5	66.8	93.9
	gravel with boulde	45	gravel with boulder	45	49.2	53.7	45.0	57.7	71.2	45.0	70.3	97.4

Figure 3 shows the difference in input motions at both ends of the building as the velocity response spectrum in a typical case. These figures show the velocity response spectrum of the input motion calculated for both ends of the 144-m long buildings in the case of a 20-degree incidence of the bearing layer. The base rock motion is a simulated seismic wave based on the Hachinohe 1968 EW phase. The peak value and the period at the peak value are different for cases (a), (b).

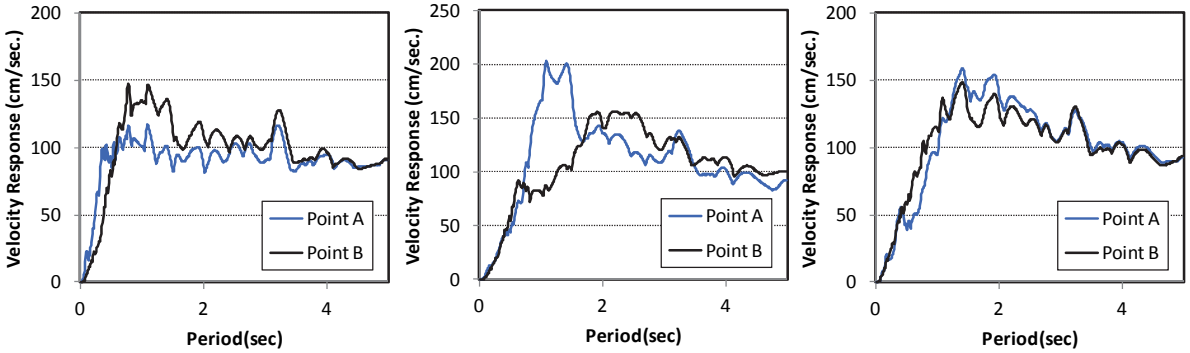

(a) Sandy stratum (b) Soft ground (c) Deep stratum with a mid-depth gravel layer

Figure 3. Velocity response spectra of the input motions at both ends of a 144-m long building based on the Hachinohe phase

3. TORSIONAL RESPONSE

3.1. Phase lag of input motion

Eighty-one response analyses were carried out for each parameter described in 2.1 and 2.2.1. Figure 4 shows the typical response time history in the case of a 144-m long building under the Hachinohe 1968 EW phase with a 50-cm/s maximum velocity, and phase lag with a 20-degree incidence angle. Figure 4a shows the time history of isolated story drift at the left end, center and right end. This difference causes the torsional response shown in Figure 4b as rotation angle time history. The torsional response leads to incremental in-story displacement at the building ends. Figure 4c shows the displacement increase ratio defined as the displacement of both ends divided by the maximum drift at the building center throughout the response time.

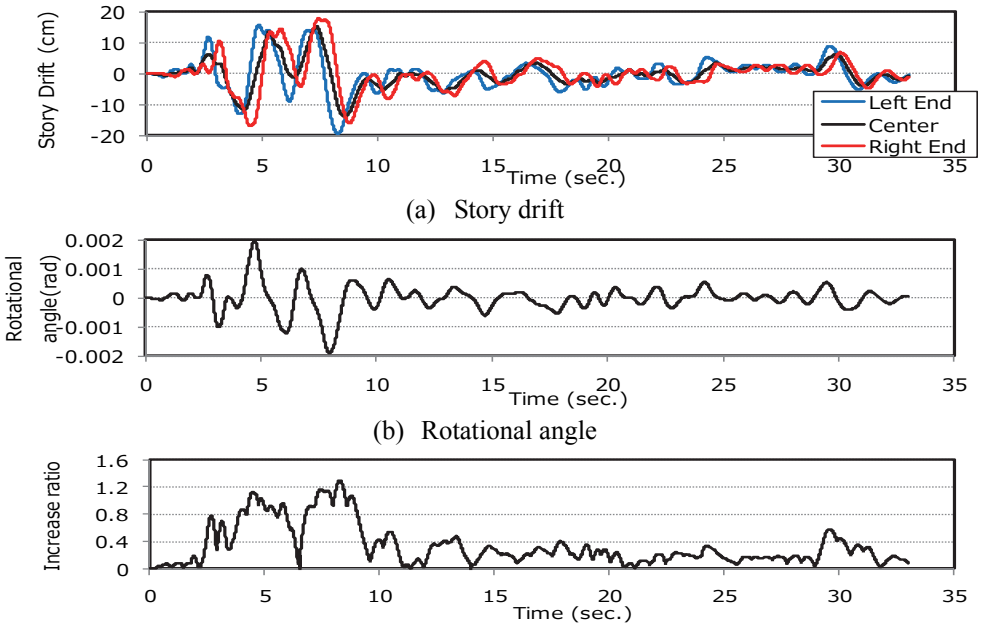

(a) Story drift

(b) Rotational angle

(c) Displacement increase ratio

Figure 4. Response of 144-m long building under Hachinohe 1968 EW phase

The maximum value is about 1.3, which occurs near the time of maximum story drift. The other calculated results show much the same pattern. Figure 5 shows the maximum displacement increase ratio for all cases.

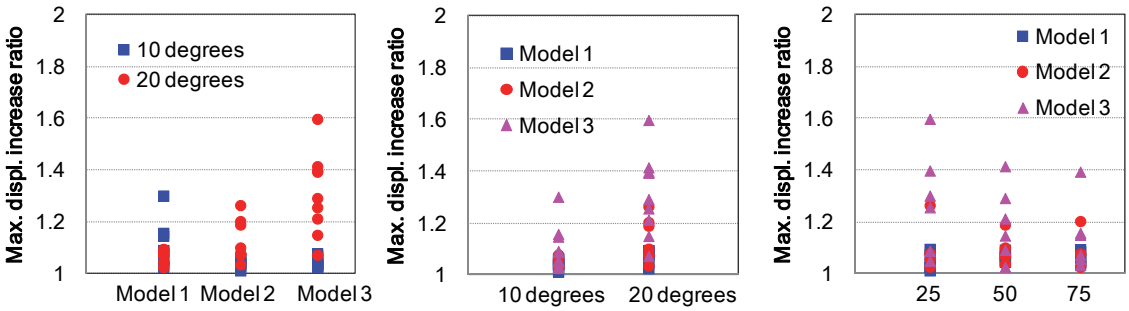

(a) Model type (b)Incidence angle (c) Input motion level

Figure 5. Displacement increase ratio

The maximum displacement increase ratio becomes larger as the building length and incidence angle increase, as shown in Figures 5a and 5b. Any difference caused by the input motion level is not observed in this study as shown in Figure 5c. The values are just less than 1.3 in most cases shown in Figures 5a and 5b. In the case of Model 3 with an incidence angle of 20 degrees, the values exceed 1.4. As the building is somewhat longer, torsional displacement tends to be larger even with the same rotation angle as Models 1 or 2.

Figure 6a shows a comparison between the calculated displacement increase ratio as described above and the estimated value calculated by the "Absolute Sum" method (ABSSUM) and the "Square Root of the Sum of Squares" method (SRSS) using the maximum story drift and rotational angle. The estimated values using ABSSUM are always larger than the calculated values. This means that the point in time when the maximum horizontal displacement occurs and when the maximum torsional rotation angle occurs is not the same. By contrast, the values using the SRSS method are less than the calculated values. As the eigen value of the horizontal and rotational modes is a closed value, the assumption for SRSS is not good. Figure 6b shows a comparison with the estimated value calculated using the "Complete Quadratic Combination" method (CQC). The correlation coefficient ρ is assumed to be 0.5 and 0.75. If this value is 1.0, it becomes ABSSUM, and if ρ =0, it is SRSS. For structural designs, it is possible to say that the estimated value using the CQC method assuming ρ >0.5 is on the safe side in this study.

$$\text{CQC method:} \quad D_{est} = \left({D_{cent}}^2 + \left(\frac{\phi \times L}{2} \right)^2 + 2 \times \rho \times D_{cent} \times \left(\frac{\phi \times L}{2} \right) \right)^{\frac{1}{2}} \tag{1}$$

here, D_{est}: estimated maximum story drift, D_{cent}: story drift at center, ϕ: rotational angle(rad), L: building length, ρ: correlation coefficient

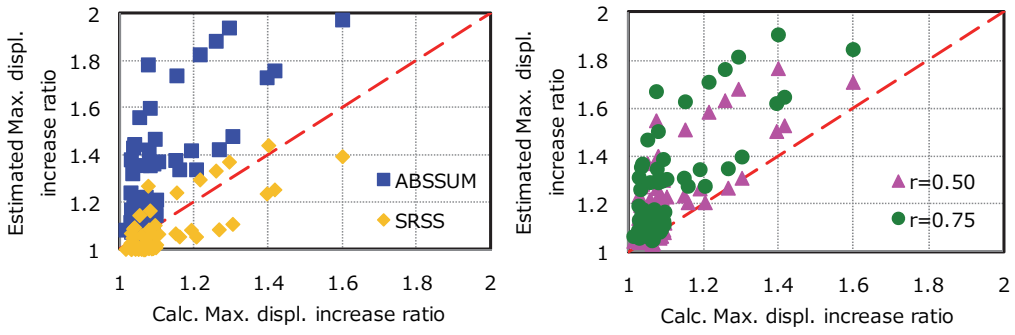

(a) Absolute Sum and SRSS method (b) CQC Method

Figure 6. Comparison between calculated and estimated displacement increase ratios

3.2. Inclination of bearing layer

Eighty-one response analyses were carried out for each parameter described in 2.1 and 2.2.2. Figure 7 shows the maximum displacement increase ratio for all cases. Figure 7a presents the results for the "Sandy stratum" case, 7b is the "Soft ground" case, and 7c is for "Deep stratum with mid-depth gravel layer". Even in the case of a 0-degree incidence angle of the bearing layer, the maximum displacement ratio is larger than 1.0, because the soil layer is not the same at both ends as shown in Table 2. The maximum displacement increase ratio becomes larger value as the building length and incidence angle increase for the "Sandy stratum" case as shown in Figure 7a; however it does not show a certain tendency for the other cases. The value is just less than 1.2 in most cases. In the case of Model 3, the maximum value is 1.25. The difference caused by the type of ground motion phase is not observed in this study, as shown in Figures a3, b3 and c3.

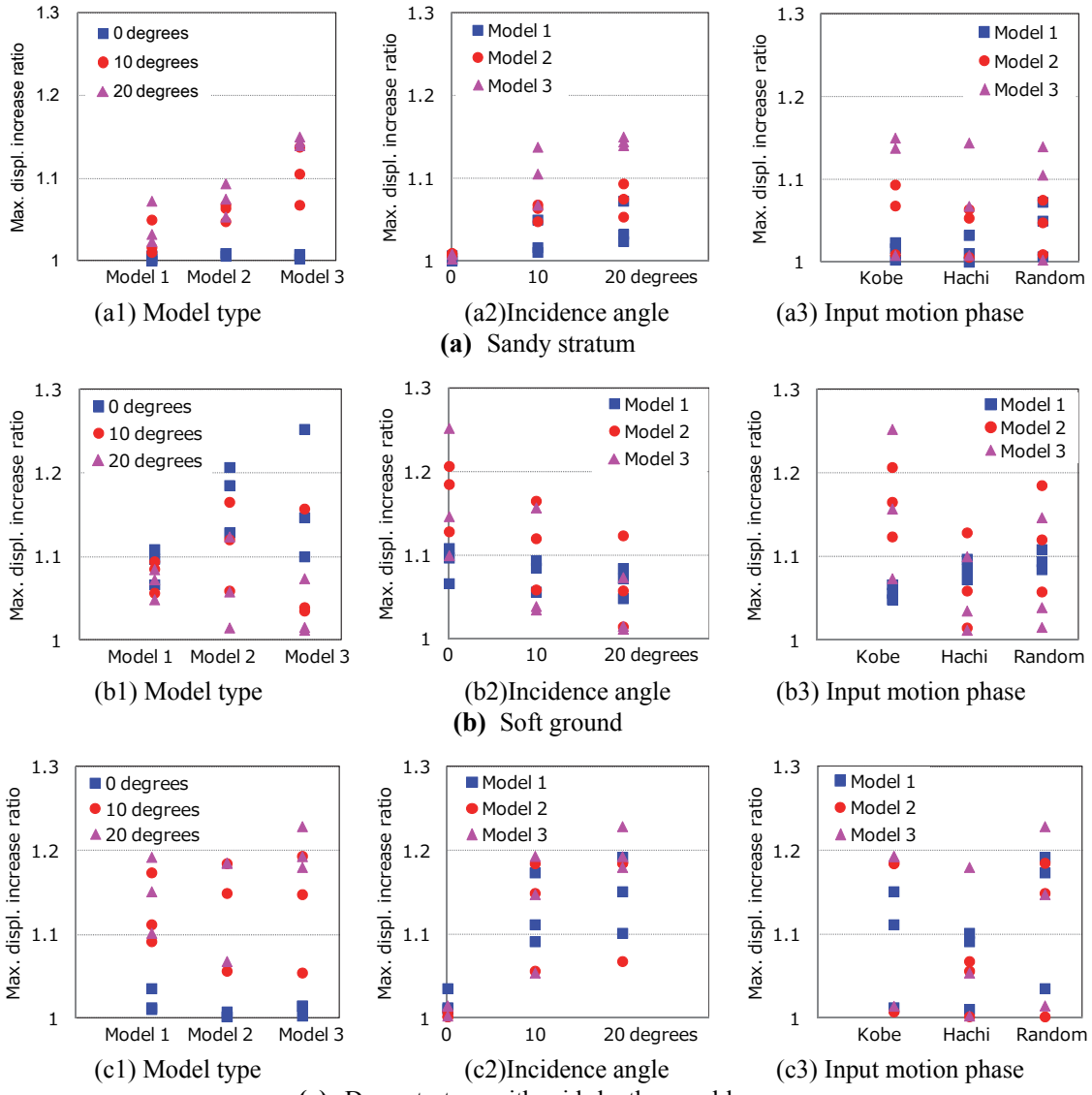

(a1) Model type (a2)Incidence angle (a3) Input motion phase

(a) Sandy stratum

(b1) Model type (b2)Incidence angle (b3) Input motion phase

(b) Soft ground

(c1) Model type (c2)Incidence angle (c3) Input motion phase

(c) Deep stratum with mid-depth gravel layer

Figure 7. Displacement increase ratio

Figure 8a shows a comparison between the calculated displacement increase ratio with ABSSUM and SRSS. The ABSSUM values are always larger than the calculated values, as opposed to the SRSS values, which are always smaller. Figure 8b shows a comparison with the CQC values with ρ =0.5 and 0.75. It is possible to say that the estimated value using the method assuming ρ >0.75 is on the safe side.

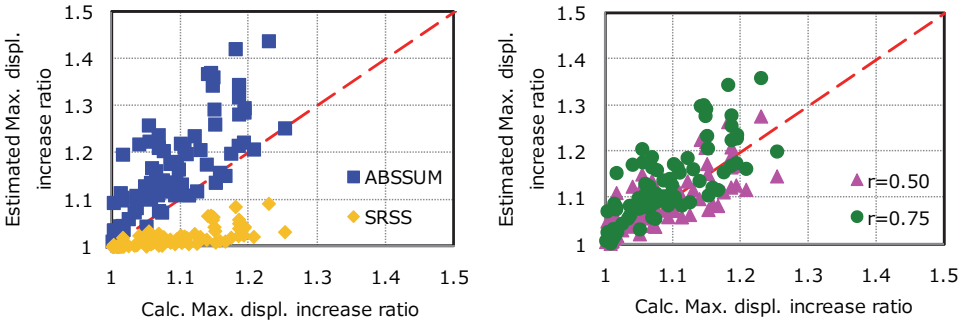

(a) Absolute Sum and SRSS method (b) CQC Method

Figure 8. Comparison between calculated and estimated displacement increase ratios

4. SIMPLE ESTIMATION OF TORSIONAL RESPONSE

4.1. Torsional response spectrum

The torsional response spectrum is calculated from the rotation angle acceleration waveform (rad/s^2) as the second derivative of the rotation angle waveform obtained from the displacement waveform difference at both ends of the building divided by the building length. The rotation angle acceleration waveform can also be calculated from the acceleration waveform difference at both ends by dividing the building length. However, for multi-input analysis, the input motion requires acceleration, velocity and displacement waveforms. In order to obtain the displacement waveform, a band-pass filter is necessary to avoid drift in one direction. Then, the original acceleration waveform was modified. In this study, the torsional response spectrum was calculated from the displacement waveform for the same condition as the multi input calculation.

Figure 9 shows a typical rotation response spectrum for the phase lag input motions. This figure shows the case where the maximum input motion level is 50-cm/s maximum velocity, the phase lag is 20 degrees, and the damping factor h is 0.10. The maximum rotation angle is different around a period of 1 second depending on the type of model (building length) and has similar values over 2 seconds. It can be called “the constant rotational response region” over a period of 2.0 seconds.

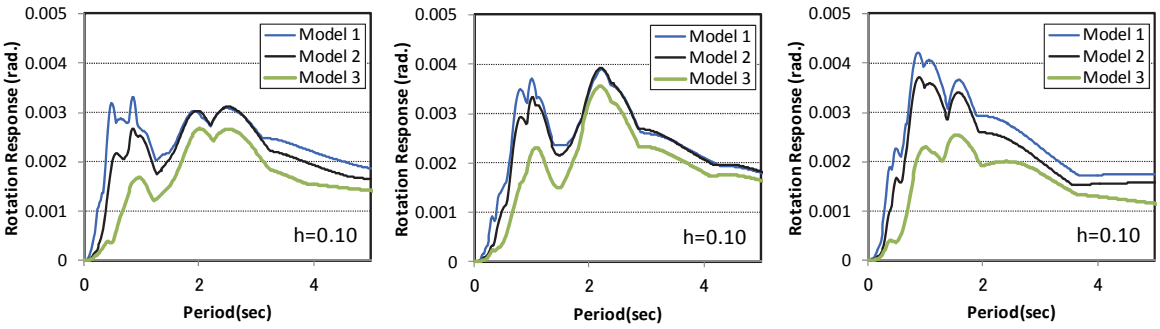

(a) El Centro 1940 NS (b) Hachinohe 1968 EW (c) Kobe 1995 NS

Figure 9. Rotation response spectra of the phase lag input motions
(Maximum level : 50-cm/s, phase lag : 20 degree)

Figure 10 shows the typical rotation response spectrum for the input motions of the inclined bearing layer. This figure shows the case where the inclined bearing layer is 20 degrees, and the damping factor h is 0.10. The maximum rotation response takes the peak value near the equivalent natural ground period. Over the peak period, rotational response moves into “the constant rotational response region”. The values for Model 1 appear different because the assumed soil layer suddenly changed within a short distance. For base-isolated buildings, the equivalent natural period during severe earthquakes is over 2 seconds, so most cases of torsional response are within “the constant rotational response region”.

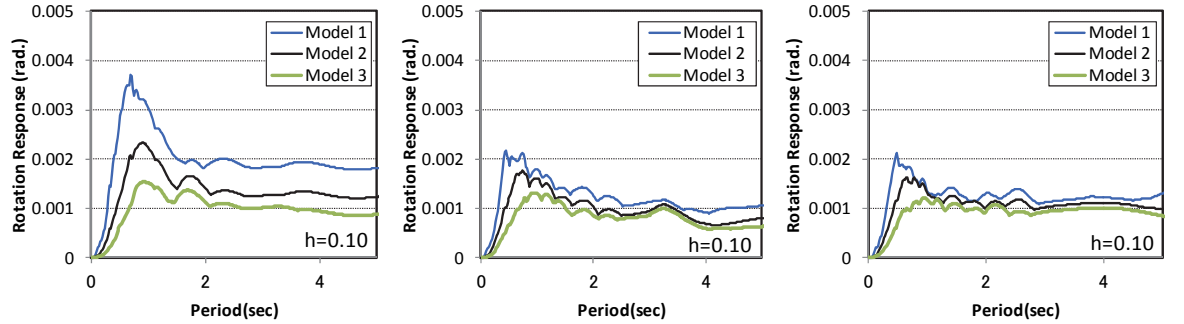

(a1) Kobe phase (a2)Hachinohe phase (a3) Random phase

(a) Sandy stratum

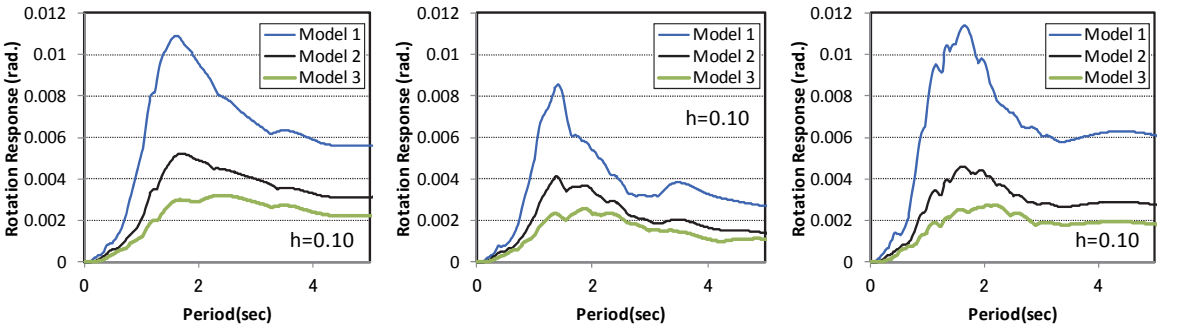

(b1) Kobe phase (b2)Hachinohe phase (b3) Random phase

(b) Soft ground

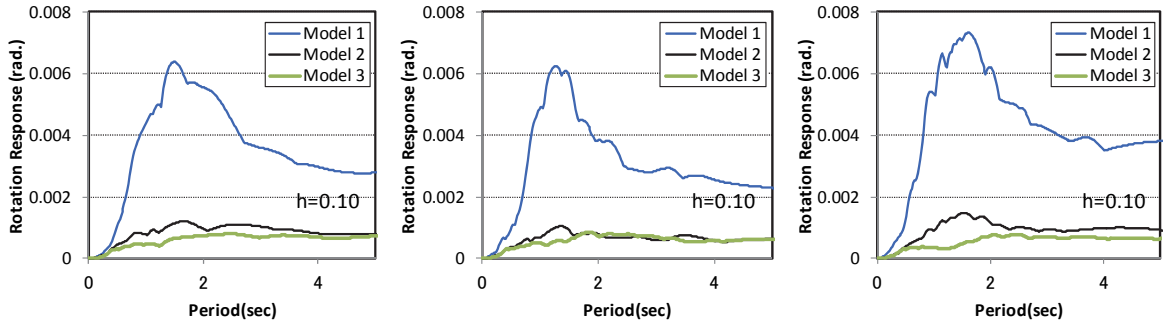

(c1) Kobe phase (c2)Hachinohe phase (c3) Random phase

(d) Deep stratum with mid-depth gravel layer

Figure 10. Rotation response spectra of input motions for the 20-degree inclined bearing layer

4.2. Estimation of torsional response by equivalent linear method

In this study, the equivalent rotational period is assumed to be equal to the horizontal equivalent period obtained from the results of a nonlinear single-input model analysis. The equivalent stiffness is calculated from the maximum response displacement and shear force of the isolation layer. The equivalent viscous damping factor was determined from Equation (2) as the standard bilinear type history loop [Ministry of Construction 2000].

$$h = 0.8 \cdot \frac{2}{\pi}\left(1 - \frac{1}{\mu}\right) \cdot \frac{(1-\alpha)}{(1+\alpha(\mu-1))} \tag{2}$$

Here, μ is the ductility factor (i.e. maximum displacement response/yielding displacement)
α is stiffness ratio (i.e. second modulus/elastic modulus)

Figure 11 shows a comparison between the calculated and estimated rotation angles. The vertical axis is the estimated rotational angle, and the horizontal axis is the rotational angle obtained from the multi-input analysis. The plotted marks are almost on the x=y line. It can be said that the rotational

angle caused by the synch motions can be estimated by equivalent linearization with the rotation response spectrum.

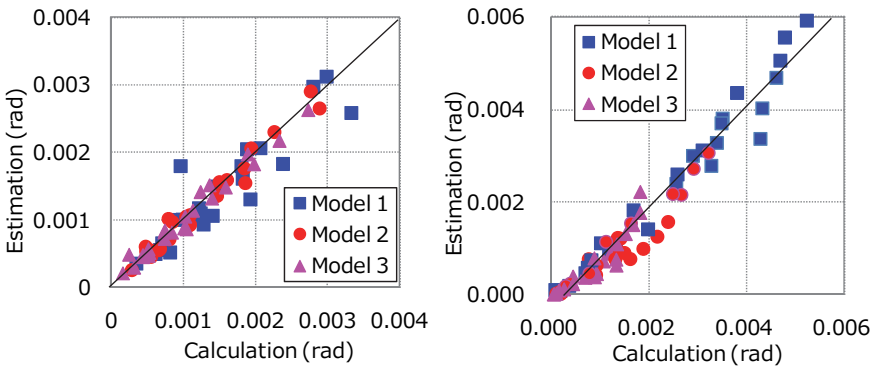

(a) Phase lag input motions (b) Inclination of bearing layer

Figure 11. Comparison between calculated and estimated rotation

4.3. Estimation of the maximum isolated story drift considering torsional motion input

From the results presented in this study, the maximum drift of an isolated story suffering torsional motion input can be estimated using the seismic response spectrum for the horizontal direction and the torsional response spectrum defined in this study as follows.

1) Calculate the horizontal drift of the isolated story using the strength response (the horizontal axis is the displacement response value and the vertical axis is the shear response for each period) and the shear-drift relationship of the isolated story using the equivalent linearization technique.
2) Using the equivalent period and the equivalent dumping factor obtained in process 1), the maximum rotational response is estimated from the torsional response spectrum.
3) The maximum isolated story drift value with torsion can be estimated from the story drift and the rotational angle using the CQC method by assuming $\rho > 0.75$

5. CONCLUSIONS

This paper examines the torsional response behavior of base-isolated buildings vibrating under varying input motions at both ends of the building defined as phase-lagged motions or motions amplified by different subsurface layer depths. The torsional response is investigated using the multi-input analysis compared to the horizontal main axial displacement. In order to approximate the torsional response, the torsional response spectrum is evaluated. The main findings are as follows:

1. The maximum displacement increase ratios are just less than 1.3 for the phase lag input motions, and are just less than 1.2 for the inclined bearing layer input motions, in most cases.
2. The rotation response spectrum has “a constant rotational response region” period of over 2 seconds in this study.
3. The maximum displacement is estimated using the CQC method while assuming $\rho > 0.75$ from the horizontal drift and the maximum rotation angle.

For practical application of the response evaluation, it is necessary to perform a more detailed discussion using the response spectrum of the torsional input.

ACKNOWLEDGMENT

Numerical calculations were conducted by Miss Kumon. I would like to express my thanks to all concerned.

REFERENCES

Ministry of Construction (2000). Notification of the Ministry of Construction, JAPAN. #2009

Shimazaki, K. (2002). Evaluation of Earthquake Resistance Ability for Base Isolated Buildings with Initial Deformation by Dry Shrinkage. *Journal of structural and construction engineering. Transactions of AIJ* **554**, 45-51.

Yamamura, K., Nishikawa, T., Nakanishi, R. (2004). Dynamic Behaviors of Structures Due to Ground Motions Considering Phase Differences. *Proceedings of the thirteenth world conference on earthquake engineering*. Paper No. 801